Pressure Induced Assembly and Coalescence of Lead Chalcogenide Nanocrystals

Lingyao Meng,[†] Sakun Duwal,[‡] J. Matthew D. Lane,[‡] Tommy Ao,[‡] Brian Stoltzfus,[‡] Marcus Knudson,[‡] Changyong Park,[§] Paul Chow,[§] Yuming Xiao,[§] Hongyou Fan*[,‡,⊥,Δ] and Yang Qin,*[,†,#]

[†] Center for Micro-Engineered Materials, University of New Mexico, Albuquerque, New Mexico 87131, USA

[‡] Sandia National Laboratories, Albuquerque, New Mexico 87123, USA

[§] HPCAT, X-ray Science Division, Argonne National Laboratories, Lemont, Illinois 60439, USA

[⊥] Department of Chemical and Biological Engineering, University of New Mexico, Albuquerque, New Mexico 87131, USA

[Δ] Center for Integrated Nanotechnology, Sandia National Laboratories, Albuquerque, New Mexico 87123, USA

[#] Department of Chemical & Biomolecular Engineering & Institute of Materials Science, University of Connecticut, Storrs, CT 06269, USA

ABSTRACT: We report here pressure induced nanocrystal coalescence of ordered lead chalcogenide nanocrystal arrays into one-dimensional (1D) and 2D nanostructures. In particular, atomic crystal phase transitions and mesoscale coalescence of PbS and PbSe nanocrystals have been observed and monitored in-situ respectively by wide- and small-angle synchrotron X-ray scattering techniques. At the atomic scale, both nanocrystals underwent reversible structural transformations from cubic to orthorhombic at significantly higher pressures than those for the corresponding bulk materials. At the mesoscale, PbS nanocrystal arrays displayed a superlattice transformation from face-centered cubic to lamellar structures, while no clear mesoscale lattice transformation was observed for PbSe nanocrystal arrays. Intriguingly, transmission electron microscopy showed that the applied pressure forced both spherical nanocrystals to coalesce into single crystalline 2D nanosheets and 1D nanorods. Our results confirm that pressure can be used as a straightforward approach to manipulate the interparticle spacing and engineer nanostructures with specific morphologies, and therefore provide insights into the design and functioning of new semiconductor nanocrystal structures under high-pressure conditions.

Recently, high pressure induced assembly has proven to be an effective method to fabricate novel functional nanomaterials.[1] Besides manipulating interatomic distances and inducing structural phase transitions at atomic scales, studies have shown that high pressure has the ability to tune inter-particle distances in nanocrystal (NC) assemblies and induce their mesoscale phase transitions and morphological changes. So far, the pressure-induced NC assembly and coalescence process has been successfully applied for synthesis of 1-3D nanostructures for various metal or semiconductor NCs.[2-16]

Lead chalcogenide (PbX, X=S or Se) NCs possess broad absorption and narrow emission bands, together with large exciton Bohr radii, making them ideal candidates for different optoelectronic applications.[17-22] Even though several investigations have been carried out,[23-27] the high-pressure behaviors of lead chalcogenide NCs have not been thoroughly understood. For example, at atomic scale, high-pressure induced structural transformation from rock-salt (RS) to orthorhombic (OR) structures has been reported for lead chalcogenide NCs with different sizes ranging from 3-30 nm.[28-33] However, phase behaviors of those NCs with even smaller sizes are not well documented. On the other hand, pressure-induced assembly and coalescence has been demonstrated for ordered arrays of 3.5 nm spherical PbS NCs[34] and 13 nm PbS nanocubes,[35] but such morphological transformation under pressure for other lead chalcogenide NCs is still unknown.

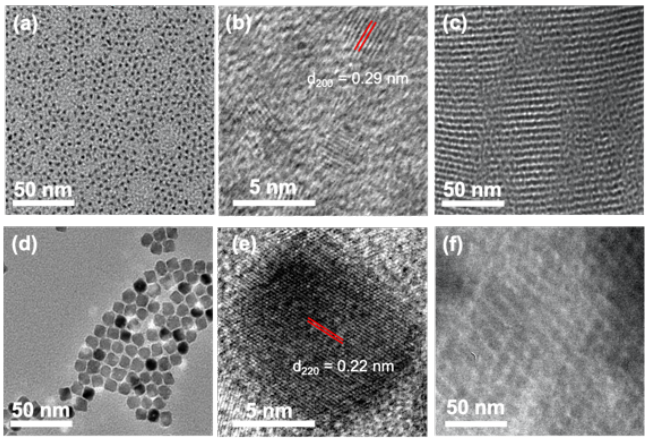

Figure 1. Morphologies of NCs before compression. (a) TEM; and (b) HRTEM images of PbS NCs; (c) TEM image of PbS

NC arrays; (d) TEM; and (e) HRTEM images of PbSe NCs; (f) TEM image of PbSe NC arrays.

Herein, we report the high-pressure behaviors of 1.6 nm PbS and 12.1 nm PbSe NCs at both the atomic and mesoscales. 1.6 ± 0.2 nm PbS and 12.1 ± 1.4 nm PbSe NCs were prepared using the hot injection method (Figures 1a and 1d).[36-37] High-resolution transmission electron microscopy (HRTEM) images revealed the (200) diffraction planes of PbS NCs (d-spacing of 0.29 nm, Figure 1b); while the fringe spacing of PbSe NCs was measured to be 0.22 nm (Figure 1e), which is in good agreement with the RS(220) plane. Ordered arrays of NCs were fabricated through slowly evaporating NC colloidal solutions on Si wafers (Figure 1c and 1f). Small pieces of the resulting films were then loaded into membrane-driven symmetric diamond-anvil cells (DACs) with silicon oil as pressure transmission medium. In-situ wide- and small-angle synchrotron X-ray scattering (WAXS/SAXS) patterns collected at ambient pressure revealed that both PbS and PbSe NCs crystallized in RS structures and assembled in face-centered cubic (fcc) mesophases. (Supporting Information, Figures S1 and S2). The samples were then gradually compressed up to 20 GPa while WAXS/SAXS measurements were carried out simultaneously at predetermined pressure points.

Figure 2 shows the in-situ WAXS and SAXS data collected for PbS sample during compression and decompression processes. At atomic scale, WAXS pattern (Figure 2a) revealed that with increasing pressure from ambient condition up to 10.46 GPa, the observed RS peaks shifted to higher q, corresponding to reduced lattice spacings as a result of unit cell contraction. Upon further compression to11.32 GPa, atomic phase transition occurred, indicated by the gradually reduced intensities of RS(220) and RS(311) peaks. At 12.69 GPa, a dramatic weakening of RS(220) and RS(311) scattering intensities was observed while the appearance of (110) and (111)/(040) peaks characteristic of the high-pressure OR phase. The onset of phase transition at 11.32 GPa is significantly higher than that reported for the bulk material (2.2 – 2.5 GPa)[38-39] and larger particles.[28] These results agree with previous reports suggesting the phase transition pressure increases with decreasing particle size due to the increase of surface energy differences between ambient and high-pressure phases.[40] The OR phase was stable up to 20 GPa, and then the pressure was gradually released. When the DAC was released back to ambient conditions, the RS phase of PbS reappeared, suggesting the pressure-induced phase transition is reversible (SI, Figure S1a). The bulk modulus for the RS phase was then calculated to be 65.35 ± 3.54 GPa by fitting the volume-*vs*-pressure curve (SI, Figure S3a) using the second-order Birch-Murnaghan equation of state,[41-42] which is higher than those reported for bulk materials (52.9 GPa).[43] Meanwhile, at the mesoscale, SAXS pattern (Figure 2b) shows a shift of peaks toward higher q as the interparticle distance decreases with increasing pressure up to a threshold pressure of 8.30 GPa. With further increasing pressure to 20 GPa, all SAXS peaks gradually shifted to lower q, suggesting the fcc structure gradually transformed to a lamellar mesophase likely caused by a deviatoric stress induced nanoparticle coalescence. The evolution of interparticle distances could be more clearly revealed in Figure S3b (SI), where the d-spacing of the first diffraction peak was plotted as a function of pressure. After the pressure was released, the lamellar structure was maintained (SI, Figure S1b).

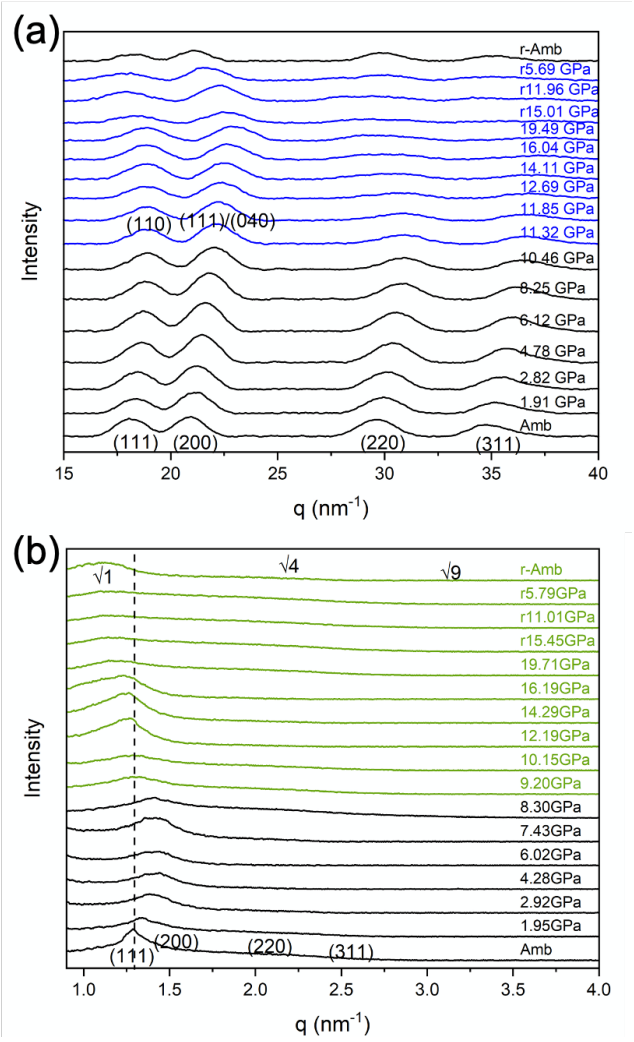

Figure 2. WAXS (a) and SAXS (b) patterns of PbS NCs during compression and decompression. "r" indicates pressure releasing. The black and blue curves in (a) represent RS and OR crystal structures, respectively; the black and green curves in (b) represent fcc and lamella superstructures, respectively.

Similarly, the high pressure WAXS and SAXS patterns for PbSe NCs are summarized in Figure 3. The WAXS patterns in Figure 3a shows that the crystal structure of PbSe NCs transformed from RS to OR at ca. 10.31 GPa, which is expectedly greater than the 4.5 GPa reported in bulk PbSe;[23] but this phase transition pressure is also higher than the 6.2 GPa observed for 8 nm NCs.[27] Such discrepancy in the size-dependent trends is most likely caused by the various pressure transmitting medium employed during the high-pressure experiments, as well as different synthesis methods leading to different capping ligands on nanoparticle surfaces. The RS to OR transition was also found to be fully reversible, and the RS bulk modulus of PbSe was calculated to be 52.49 ± 5.12 GPa (SI, Figure S4a), larger than that in bulk (45.0 GPa).[44] On the other hand, the SAXS peaks in Figure 3b shift to higher q with increasing pressures up to 13.22 GPa, followed by blue-shift to lower q upon further compression, suggesting a pressure induced assembly and coalescence of neighboring NCs. Unlike the mesoscale phase transition observed in the PbS case, the d-spacing of the first SAXS peak of PbSe arrays return to the initial value when pressure is released back to ambient (SI, Figure S4b). The recovered SAXS

peaks are found to be slightly broader and no obvious peak position shift when compared to those before compression (SI, Figure S2b).

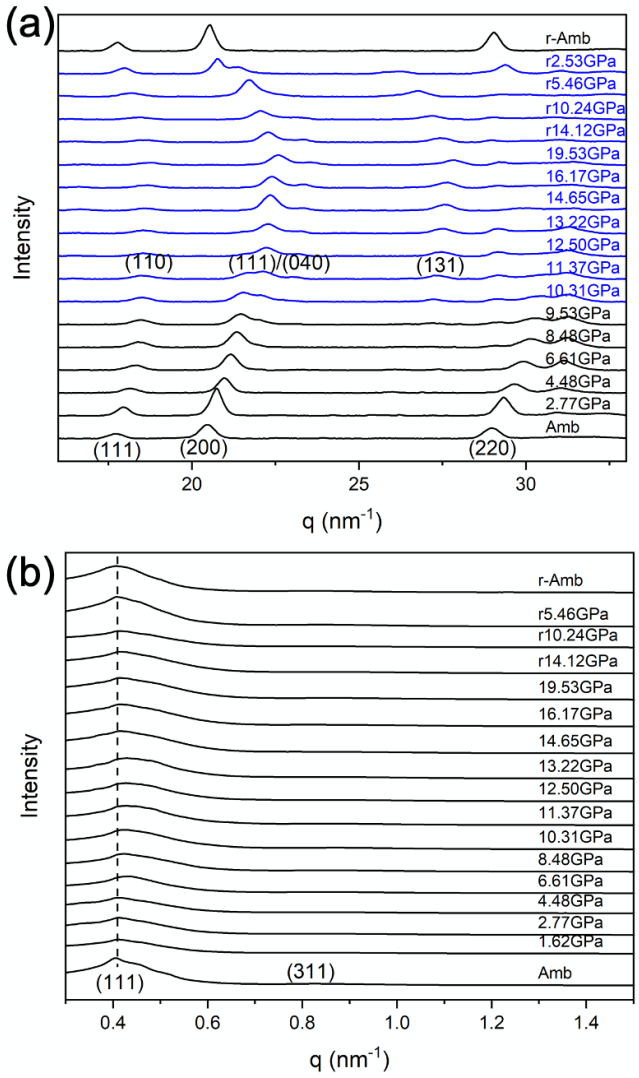

Figure 3. WAXS (a) and SAXS (b) patterns of PbSe NCs during compression and decompression. "r" indicates the releasing pressure. The black and blue curves in (a) represent RS and OR crystals structures

To confirm the pressure induced NC coalescence suggested by SAXS measurements, TEM was conducted for samples after compression. In the case of PbS NCs, formation of 2D nanosheets is observed (Figure 4a and Figure S5a of SI). The insert image in Figure 4a shows a typical lamellar structure with the width of the edge-on lamella at ~1.65 nm, in agreement with the particle size and SAXS measurements. Such orientated coalescence of neighboring NCs into nanosheets has been previously reported for 3.5 nm PbS NCs and the atomic and meso scale transitions were found to occur at the same pressure.[34] However, in our case, the phase transition pressure at the mesoscale is significantly lower than that found at the atomic scale. Besides the differences in experimental setup, where no pressure transmitting medium was used in the previous study,[34] we also attribute this inconsistent observation to the overwhelming high surface energy of very small particles. The combined effects of stronger quantum confinement at atomic scale and greater sintering tendency at mesoscale eventually trigger the coalescence of smaller NCs at lower pressure. Previous research also suggests that both RS(200) and RS(220) guide the orientation of the attachment;[34] while in the current study, uniform lattice fringes in HRTEM images match the spacing between (220) planes of PbS in RS phase (Figure 4b and Figure S5b of SI). In addition, we observed the formation of short nanowires. The average diameter of nanowire is about 2.1 ± 0.4 nm, slightly larger than the diameter of initial particles. The lattice fringe of 0.28 nm corresponds to the RS(200) plane (Figures 2c and 2d).

We hypothesize that, at ambient condition, NCs in fcc arrays are isotopically oriented with balanced NC interactions, but their ligand covered RS{111} facets have lower surface energy than RS{200} and RS{220} facets.[45] Below 9.0 GPa, ligands on the NC surfaces provide sufficient compressibility to maintain their mesoscale assemblies and NCs cannot move freely. When pressure is increased to higher than 9.0 GPa, silicon oil could no long provide a hydrostatic compression environment.[46-47] Compression of the superlattice then produces a deviatoric stress along the mesoscale <110> direction (parallel to the compression axis). Such nonequilibrium deformation breaks the local force balance between NCs and promotes their relocation and reorientation. The high pressure deviatoric stress acts as the driving force to firstly detach ligands from NC surfaces, and then rotate, attach, and coalesce the NCs along (220) planes into single crystal nanosheets to reduce surface energy and induce mesoscale phase transition, similar to the attachment model proposed previously.[34] Upon further increasing pressure to the NC atomic phase transition region, the structural transformation results in exposing nanostructures to the high energy OR phase, which requires greater driving force to enable the rotation of NCs, consequently slowing down the orientated attachment process. As a result, the NCs directly fuse into short nanowires. Another hypothesis could be that the observed short nanowires were the intermediate step in the nanosheet formation. Further TEM analysis on samples at different pressure stage would be needed to verify the above theories.

For PbSe NCs, long nanorods are observed after compression with lengths up to 150 nm and diameters at 14.5 ± 2.1 nm that is similar to the sizes of starting NCs (Figures 4e and 4g). To the best of our knowledge, this is the first pressure-induced sintering reported for PbSe NCs. Markedly, HRTEM images revealed that the nanorods are single crystalline with both (200) and (220) planes preferentially oriented (Figures 4f and 4h; Figure S6, SI). Such observations on sintering of nanospheres to nanorods have been reported for various nanoparticles, and the mechanism has been generally explained by the occurrence of nonhydrostatic stress upon increasing pressure which can break the balanced force between neighboring NCs and force them to sinter into continued nanorods.[1] However, this observed NC coalescence is not universal, a large number of free particles still exist (SI Figures 6 (e) and (f)), which explains the insignificant peak shift in the recovered SAXS spectrum after release of pressure. The size of the non-sintered NCs was measured to be 12.6 ± 1.6 nm. We suspect the lack of clear SAXS mesophase transition was related to NCs size effect, as larger particles (more than 10 nm) have been found to sinter slower and less than the higher surface energy and smaller particles.[48-49] CdS NCs has also been reported to have such size dependent sintering behavior under pressure.[10]

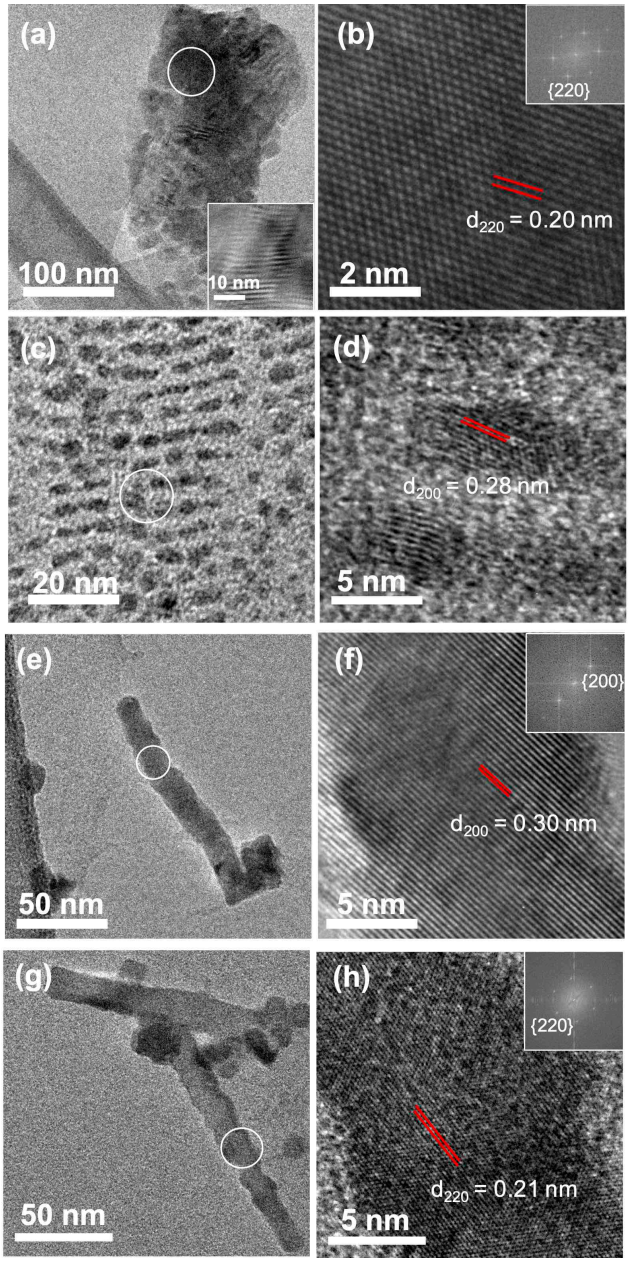

Figure 4. Morphologies of NCs after compression: (a) TEM images of 2D PbS nanosheet and lamellar structures (inset); (b) HRTEM image of the circled area in (a) and the corresponding Fast-Fourier transformation (FFT) pattern (inset); (c-d) TEM and HRTEM images of 1D PbS short nanowires; (e-h) TEM, HRTEM and FFT (inset) images of 1D PbSe nanorods.

In conclusion, we demonstrated here that pressure can be successfully applied to fabricate both 1D and 2D lead chalcogenide nanostructures. By combined high pressure-SAXS/WAXS experiments with TEM analysis, we found the sintering of initially small PbS NCs into 2D nanosheets. Comparing to previous reports, the unusual observation of higher atomic scale phase transition than mesoscale phase transition observed here also results in the formation of 1D short nanowires. In addition, coalescence of 12.1 nm PbSe NCs into nanorods was observed, which represents the first example of pressure-driven morphology engineering of PbSe NCs. This high-pressure fabrication technique is still at its early development stage with many possibilities for future research, and we expect it to be applied to a large variety of nanoparticles that contain both amorphous and crystalline phases and to achieve large-scale sample preparation for desired applications.

ASSOCIATED CONTENT

Supporting Information

Experimental details and additional data. The Supporting Information is available free of charge on the ACS Publications website.

AUTHOR INFORMATION

Corresponding Author

* hfan@sandia.gov
* yang.qin@uconn.edu

ACKNOWLEDGMENT

Y.Q. thanks the National Science Foundation (DMR-1453083 and CHE-1904659) for supporting this work. This work was supported by the Sandia's Laboratory Directed Research & Development (LDRD) program. Portions of this work were performed at HPCAT (Sector 16), Advanced Photon Source (APS), Argonne National Laboratory. HPCAT operations are supported by DOE-NNSA's Office of Experimental Sciences. The Advanced Photon Source is a U.S. Department of Energy (DOE) Office of Science User Facility operated for the DOE Office of Science by Argonne National Laboratory under Contract No. DE-AC02-06CH11357. This paper describes objective technical results and analysis. Any subjective views or opinions that might be expressed in the paper do not necessarily represent the views of the U.S. DOE or the United States Government. Research was carried out, in part, at the Center of Integrated Nanotechnology (CINT), a US Department of Energy, Office of Basic Energy Sciences user facility. Sandia National Laboratories is a multimission laboratory managed and operated by National Technology and Engineering Solutions of Sandia, LLC., a wholly owned subsidiary of Honeywell International, Inc., for the U.S. Department of Energy's National Nuclear Security Administration under contract DE-NA0003525

REFERENCES

(1) Bai, F.; Bian, K.; Huang, X.; Wang, Z.; Fan, H., Pressure induced nanoparticle phase behavior, property, and applications. *Chem. Rev.* **2019**, *119*, 7673-7717.
(2) Wu, H.; Bai, F.; Sun, Z.; Haddad, R. E.; Boye, D. M.; Wang, Z.; Fan, H., Pressure-Driven Assembly of Spherical Nanoparticles and Formation of 1D-Nanostructure Arrays. *Angew. Chem.* **2010**, *122*, 8609-8612.
(3) Wu, H.; Bai, F.; Sun, Z.; Haddad, R. E.; Boye, D. M.; Wang, Z.; Huang, J. Y.; Fan, H., Nanostructured gold architectures formed through high pressure-driven sintering of spherical nanoparticle arrays. *J. Am. Chem. Soc.* **2010**, *132*, 12826-12828.
(4) Li, B.; Bian, K.; Lane, J. M. D.; Salerno, K. M.; Grest, G. S.; Ao, T.; Hickman, R.; Wise, J.; Wang, Z.; Fan, H., Superfast assembly and synthesis of gold nanostructures using nanosecond low-temperature compression via magnetic pulsed power. *Nat. Commun.* **2017**, *8*, 1-9.
(5) Wu, H.; Wang, Z.; Fan, H., Stress-induced nanoparticle crystallization. *J. Am. Chem. Soc.* **2014**, *136*, 7634-7636.
(6) Li, W.; Fan, H.; Li, J., Deviatoric stress-driven fusion of nanoparticle superlattices. *Nano Lett.* **2014**, *14*, 4951-4958.
(7) Li, B.; Wen, X.; Li, R.; Wang, Z.; Clem, P. G.; Fan, H., Stress-induced phase transformation and optical coupling of silver nanoparticle superlattices into mechanically stable nanowires. *Nat. Commun.* **2014**, *5*, 1-7.
(8) Zhu, J.; Quan, Z.; Wang, C.; Wen, X.; Jiang, Y.; Fang, J.; Wang, Z.; Zhao, Y.; Xu, H., Structural evolution and mechanical

behaviour of Pt nanoparticle superlattices at high pressure. *Nanoscale* **2016**, *8*, 5214-5218.
(9) Meng, L.; Lane, J. M. D.; Baca, L.; Tafoya, J.; Ao, T.; Stoltzfus, B.; Knudson, M.; Morgan, D.; Austin, K.; Park, C., Shape Dependence of Pressure-Induced Phase Transition in CdS Semiconductor Nanocrystals. *J. Am. Chem. So*c. **2020**, *142*, 6505-6510.
(10) Meng, L.; Fan, H.; Lane, J. M.; Baca, L.; Tafoya, J.; Ao, T.; Stoltzfus, B.; Knudson, M.; Morgan, D.; Austin, K., X-Ray Diffraction and Electron Microscopy Studies of the Size Effects on Pressure-Induced Phase Transitions in CdS Nanocrystals. *MRS Adv.* **2020**, *5*, 2447-2455.
(11) Li, B.; Bian, K.; Zhou, X.; Lu, P.; Liu, S.; Brener, I.; Sinclair, M.; Luk, T.; Schunk, H.; Alarid, L., Pressure compression of CdSe nanoparticles into luminescent nanowires. *Sci. Adv.* **2017**, *3*, e1602916.
(12) Wang, Z.; Wen, X.-D.; Hoffmann, R.; Son, J. S.; Li, R.; Fang, C.-C.; Smilgies, D.-M.; Hyeon, T., Reconstructing a solid-solid phase transformation pathway in CdSe nanosheets with associated soft ligands. *Proc. Natl. Acad. Sci. U.S.A*. **2010**, *107*, 17119-17124.
(13) Liu, H.; Yang, X.; Wang, K.; Wang, Y.; Wu, M.; Zuo, X.; Yang, W.; Zou, B., Pressure-Induced Multidimensional Assembly and Sintering of CuInS2 Nanoparticles into Lamellar Nanosheets with Band Gap Narrowing. *ACS Appl. Nano Mater.* **2020**, *3*, 2438-2446.
(14) Zhu, H.; Nagaoka, Y.; Hills-Kimball, K.; Tan, R.; Yu, L.; Fang, Y.; Wang, K.; Li, R.; Wang, Z.; Chen, O., Pressure-enabled synthesis of hetero-dimers and hetero-rods through intraparticle coalescence and interparticle fusion of quantum-dot-Au satellite nanocrystals. *J. Am. Chem. Soc.* **2017**, *139*, 8408-8411.
(15) Zhu, H.; Cai, T.; Yuan, Y.; Wang, X.; Nagaoka, Y.; Zhao, J.; Liu, Z.; Li, R.; Chen, O., Pressure-Induced Transformations of Three-Component Heterostructural Nanocrystals with CdS–Au2S Janus Nanoparticles as Hosts and Small Au Nanoparticles as Satellites. *ACS Appl. Nano Mater.* **2019**, *2*, 6804-6808.
(16) Nagaoka, Y.; Hills-Kimball, K.; Tan, R.; Li, R.; Wang, Z.; Chen, O., Nanocube superlattices of cesium lead bromide perovskites and pressure-induced phase transformations at atomic and mesoscale levels. *Adv. Mater.* **2017**, *29*, 1606666.
(17) Talapin, D. V.; Lee, J.-S.; Kovalenko, M. V.; Shevchenko, E. V., Prospects of colloidal nanocrystals for electronic and optoelectronic applications. *Chem. Rev.* **2010**, *110*, 389-458.
(18) Sun, L.; Choi, J. J.; Stachnik, D.; Bartnik, A. C.; Hyun, B.-R.; Malliaras, G. G.; Hanrath, T.; Wise, F. W., Bright infrared quantum-dot light-emitting diodes through inter-dot spacing control. *Nat. Nanotechnol.* **2012**, *7*, 369-373.
(19) Ma, X.; Xu, F.; Benavides, J.; Cloutier, S. G., High performance hybrid near-infrared LEDs using benzenedithiol cross-linked PbS colloidal nanocrystals. *Org. Electron.* **2012**, *13*, 525-531.
(20) Choi, J. J.; Lim, Y.-F.; Santiago-Berrios, M. E. B.; Oh, M.; Hyun, B.-R.; Sun, L.; Bartnik, A. C.; Goedhart, A.; Malliaras, G. G.; Abruna, H. D., PbSe nanocrystal excitonic solar cells. *Nano Lett.* **2009**, *9*, 3749-3755.
(21) Etgar, L.; Moehl, T.; Gabriel, S.; Hickey, S. G.; Eychmüller, A.; Grätzel, M., Light energy conversion by mesoscopic PbS quantum dots/TiO2 heterojunction solar cells. *ACS Nano* **2012**, *6*, 3092-3099.
(22) Rafailov, E. U.; Cataluna, M. A.; Sibbett, W., Mode-locked quantum-dot lasers. *Nat. Photonics* **2007**, *1*, 395-401.
(23) Chattopadhyay, T.; Von Schnering, H.; Grosshans, W.; Holzapfel, W., High pressure X-ray diffraction study on the structural phase transitions in PbS, PbSe and PbTe with synchrotron radiation. *Physica B+ C* **1986**, *139*, 356-360.
(24) Bian, K.; Wang, Z.; Hanrath, T., Comparing the structural stability of PbS nanocrystals assembled in fcc and bcc superlattice allotropes. *J. Am. Chem. Soc.* **2012**, *134*, 10787-10790.
(25) Zhuravlev, K. K.; Pietryga, J. M.; Sander, R. K.; Schaller, R. D., Optical properties of PbSe nanocrystal quantum dots under pressure. *Appl. Phys. Lett*. **2007**, *90*, 043110.
(26) Lin, Y.-C.; Chou, W.-C.; Susha, A. S.; Kershaw, S. V.; Rogach, A. L., Photoluminescence and time-resolved carrier dynamics in thiol-capped CdTe nanocrystals under high pressure. *Nanoscale* **2013**, *5*, 3400-3405.
(27) Joy, K. F.; Jaya, N. V. Resistivity Measurement of Nanocrystalline Lead Selenide Under High Pressure. *InProc Indian Natn Sci Acad*, **2013**, *79*, 391-393.
(28) Podsiadlo, P.; Lee, B.; Prakapenka, V. B.; Krylova, G. V.; Schaller, R. D.; Demortiere, A.; Shevchenko, E. V., High-pressure structural stability and elasticity of supercrystals self-assembled from nanocrystals. *Nano Lett.* **2011**, *11*, 579-588.
(29) Bian, K.; Richards, B. T.; Yang, H.; Bassett, W.; Wise, F. W.; Wang, Z.; Hanrath, T., Optical properties of PbS nanocrystal quantum dots at ambient and elevated pressure. *Phys. Chem. Chem. Phys* **2014**, *16*, 8515-8520.
(30) Qadri, S. B.; Yang, J.; Ratna, B.; Skelton, E. F.; Hu, J., Pressure induced structural transitions in nanometer size particles of PbS. *Appl. Phys. Lett.* **1996**, *69*, 2205-2207.
(31) Jiang, J.; Gerward, L.; Secco, R.; Frost, D.; Olsen, J.; Truckenbrodt, J., Phase transformation and conductivity in nanocrystal PbS under pressure. *J. Appl. Phys.* **2000**, *87*, 2658-2660.
(32) Freny Joy, K.; Victor Jaya, N.; Zhu, J.-J., Structural transformation in PbS and HgS nanocrystals under high pressure. *Mod. Phys. Lett. B* **2006**, *20*, 963-970.
(33) Bian, K.; Bassett, W.; Wang, Z.; Hanrath, T., The strongest particle: size-dependent elastic strength and Debye temperature of PbS nanocrystals. *J. Phys. Chem. Lett.* **2014**, *5*, 3688-3693.
(34) Wang, Z.; Schliehe, C.; Wang, T.; Nagaoka, Y.; Cao, Y. C.; Bassett, W. A.; Wu, H.; Fan, H.; Weller, H., Deviatoric stress driven formation of large single-crystal PbS nanosheet from nanoparticles and in situ monitoring of oriented attachment. *J. Am. Chem. Soc.* **2011**, *133*, 14484-14487.
(35) Wang, T.; Li, R.; Quan, Z.; Loc, W. S.; Bassett, W. A.; Xu, H.; Cao, Y. C.; Fang, J.; Wang, Z., Pressure processing of nanocube assemblies toward harvesting of a metastable PbS phase. *Adv. Mater*. **2015**, *27*, 4544-4549.
(36) Hines, M. A.; Scholes, G. D., Colloidal PbS nanocrystals with size-tunable near-infrared emission: observation of post-synthesis self-narrowing of the particle size distribution. *Adv. Mater*. **2003**, *15*, 1844-1849.
(37) Li, H.; Chen, D.; Li, L.; Tang, F.; Zhang, L.; Ren, J., Size-and shape-controlled synthesis of PbSe and PbS nanocrystals via a facile method. *CrystEngComm* **2010**, *12*, 1127-1133.
(38) Wakabayashi, I.; Kobayashi, H.; Nagasaki, H.; Minomura, S., The effect of pressure on the lattice parameters Part I. PbS and PbTe Part II. Gd, NiO, and α-MnS. *J. Phys. Soc. Japan* **1968**, *25*, 227-233.
(39) Lin, J.-C.; Sharma, R.; Chang, Y., The Pb− S (Lead-Sulfur) system. *Bulletin of Alloy Phase Diagrams* **1986**, *7*, 374.
(40) Tolbert, S. H.; Alivisatos, A., High-pressure structural transformations in semiconductor nanocrystals. *Annu. Rev. Phys. Chem*. **1995**, *46,* 595-626.
(41) Murnaghan, F. D., Finite deformations of an elastic solid. *Am. J. Math.* **1937**, *59*, 235-260.
(42) Murnaghan, F., The compressibility of media under extreme pressures. *Proc. Natl. Acad. Sci. U.S.A* **1944**, *30*, 244.
(43) Knorr, K.; Ehm, L.; Hytha, M.; Winkler, B.; Depmeier, W., The high-pressure α/β phase transition in lead sulphide (PbS). *Eur. Phys. J. B* **2003**, *31*, 297-303.
(44) Wang, S.; Zang, C.; Wang, Y.; Wang, L.; Zhang, J.; Childs, C.; Ge, H.; Xu, H.; Chen, H.; He, D., Revisit of pressure-induced phase transition in PbSe: crystal structure, and thermoelastic and electrical properties. *Inorg. Chem*. **2015**, *54*, 4981-4989.

(45) Fang, C.; van Huis, M. A.; Vanmaekelbergh, D.; Zandbergen, H. W., Energetics of polar and nonpolar facets of PbSe nanocrystals from theory and experiment. *ACS Nano* **2010**, *4*, 211-218.
(46) Ragan, D. D.; Clarke, D. R.; Schiferl, D., Silicone fluid as a high-pressure medium in diamond anvil cells. *Rev. Sci. Instrum*. **1996**, *67*, 494-496.
(47) Guo, Q.; Zhao, Y.; Mao, W. L.; Wang, Z.; Xiong, Y.; Xia, Y., Cubic to tetragonal phase transformation in cold-compressed Pd nanocubes. *Nano Lett*. **2008**, *8*, 972-975.

For Table of Contents Only

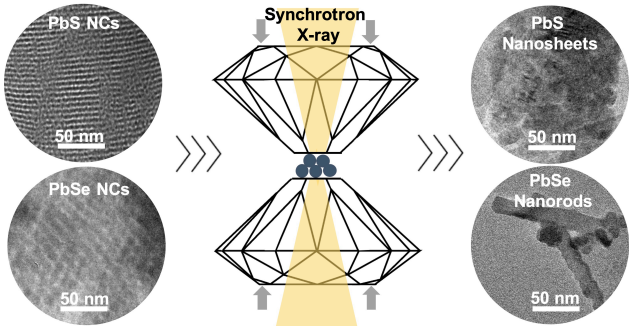

(48) German, R., T*hermodynamics of sintering. In Sintering of advanced materials*, Elsevier: 2010; pp 3-32.
(49) Guozhong, C., *Nanostructures and nanomaterials: synthesis, properties and applications*. World scientific: 2004; pp 17-26.